Proceedings of the Korean Nuclear Society Spring Meeting
Kwangju, Korea, May 2002

Evaluation of Heating Rates for CEA, ICI and NSA for KSNP

Yong Il Kim, Joon Gi Ahn and Hae Ryong Hwang

Korea Power Engineering Company, Inc.
150 Duckjin, Yusong
Daejeon, Korea 305-353

Abstract

Radiation heating rates to the instruments located in the guide tubes of fuel assembly are required for the cooling analysis in the field of reactor core thermohydraulics. Previous evaluation of heating rates for the ABB-CE type power plants has been used for the design data for KSNP. But there are some differences in the structures and component materials of the instruments between them. So, it is necessary to re-evaluate the heating rates for the instruments using up-to-date cross-section library and transport code to see whether the previous evaluations are suitable for KSNP or not. The evaluations of heating rates in each component of the instruments have been performed by MCNP code and the results have been compared to those of previous works.

1. Introduction

In 1970s, heating rate calculations had been performed by Combustion Engineering for Control Element Assembly (CEA), In-Core Instrumentation (ICI) and Neutron Source Assembly (NSA) for Arkansas[1], St. Lucie 2[2] and System 80[3] reactors. The values of heating rate from those calculations have been employed in the cooling analysis for KSNP. The previous methodology for CEA heating rate calculation was very complicated and depended largely on hand calculations due to the limitations of computing environments for those days. For other instruments such as ICI and NSA, heating rate results had been provided but specific calculational methods were not available. Therefore it is necessary to evaluate the heating rates in the CEA, ICI and NSA for KSNP by using up-to-date cross section library and

transport code.

The neutron and photon transport calculations have been done by MCNP4B[4] code which is based on Monte Carlo transport methodology. Continuous energy neutron data based on ENDF/B-VI and photon interaction data have been employed for the nuclear cross-sections of the transport calculations. Neutron and photon heating rates have been obtained from track length estimates of energy depositions.

2. Calculational Methodology

The previous calculational methodology for CEA heating rate is based on the heating factors classified by their origins of heating due to neutron absorption, prompt particles and delayed gammas. The heating factors are then multiplied by neutron absorption rate, neighboring fuel pin powers, or pin peaking factor depending on the origins of heating. It is mentioned that the previous heating rate calculation for ICI and NSA employ Monte Carlo method but detailed description for the methodology is not available. Therefore the description of previous calculational methodology will be focused on the CEA heating rate calculation.

To evaluate heating rates in the components of CEA, ICI and NSA for KSNP, one Fuel Assembly (FA) which includes all the instruments is modeled and the particle transport calculation are performed by MCNP4B code. The boundaries of calculation model are constructed as follows; lateral sides of an active fuel assembly region are surrounded by reflecting surfaces, and mixtures of steel and coolant are placed on bottom and top faces of fuel assembly. To include the heating from delayed gammas produced from fission reaction, additional heating rates calculation using delayed gamma spectrum as source distribution is performed and the results are added on the prompt particle calculation results. The heating rates of each component are obtained from track length estimate of cell energy deposition tally[4] for neutron and photon.

2.1. Previous CEA Heating Rate Calculation

Heating in CEA consists of two major contributing components: neutron absorption heating (E_n) and environmental heating (E_e). The environmental heating is composed of both prompt and delayed components (E_p and E_d). The heating is originated from following three major sources:

a. Heating from neutron absorption

The maximum axially averaged neutron absorption heating is equal to

$$E_n = e_n \times R_n \times F_n$$

where e_n in is the energy released in the CEA material by the absorption of one neutron in the rod cell, R_n is the average neutron absorption rate for the CEA region, and F_n is maximum to average absortion rate for all inserted CEA fingers.

b. Heating from prompt particles

The maximum axially averaged prompt particle heating is equal to

$$E_p = e_p \times W_c$$

where e_p is the energy deposited by the prompt particle at a local power density of 1.0 W/cc and W_c is the local core power density in W/cc. Note that W_c is equal to

$$W_c = PD \times PL \times P_{max}/RPD$$

where PD is core average power density in W/cc, and PL is the average relative power density of the 12 fuel pins surrounding each rodded waterhole, and P_{max}/RPD is highest value of maximum pin to box factor in the rodded boxes.

c. Heating from delayed gammas

The maximum axially averaged heating from delayed gamma generated by the decay of the fission product is calculated by

$$E_d = e_d \times PD \times F_L$$

where e_d is the energy deposited by the delayed gammas at a local power density of 1.0 W/cc, PD is core average power density in W/cc, and F_L is pre-insertion 1-pin radial peaking factor in rodded boxes.

The heating rate of a material composing the CEA and surrounding component is the sum of the above three heating rates and the total heating rate of CEA or surrounding component is the sum of heating rates of materials as follows:

$$E = \sum_{i=1} E^i = \sum_{i=1} (E_n^i + E_p^i + E_d^i)$$

where E is the total heating rate and E^i is the heating rate of material i.

The heating factors due to neutron absorption (e_n), prompt particles (e_p) and delayed gammas (e_d) were obtained from the calculation[1] for the Arkansas reactor

and they were applied to CEA heating rate calculation for YGN 3&4 .

In order to calculate the CEA heating rates, not only heating factors but also node-wise power density and fluxes are required. From the YGN 3&4 core calculation, node-wise information for Bank 5 (full strength CEA) and/or part strength CEA (PSCEA) insertion cases were conservatively examined[5]. Therefore maximum node power and fluxes of assemblies in which lead bank and PSCEA are to be inserted were chosen as shown in Table 1.

2.2. MCNP Calculations for CEA, ICI and NSA

The KSNP reactor[6] core consists of 177 fuel assemblies. Each fuel assembly consists of a 16316 array of 236 fuel rods, 4 guide tubes (GT) for control rod , and an in-core instrumentation guide tube as shown in Figure 1.

For simplicity of modeling and calculation, it is assumed that all instruments are located in one fuel assembly. Figure 2 shows the MCNP calculation model which includes CEAs, ICI and NSA in one fuel assembly. As shown in Figure 2, ICI and NSA are placed in the guide tubes of center and lower right while CEA and PSCEA are inserted in the guide tubes of upper and lower left respectively. Reflecting boundary condition is applied to four lateral sides of the FA and mixture zones are placed above and below the active fuel region to take into account reflecting particles. Vacuum boundary condition is applied to the bottom and top sides of the model. The CEA and PSCEA are fully inserted to maximize heating rates in the components of CEAs.

The source definitions for space and energy are input by using standard source variables in a general source card for MCNP input. A cylindrical volume distribution for a fuel rod is defined for the sampling of position of particles with the application of uniform radial and axial source distributions. Equal sampling probability is given to all 236 fuel rods in a FA so as to perform even sampling for all fuel rods. One of the built-in functions for source probability in MCNP code, Watt fission neutron energy spectrum is chosen for the source energy distribution as

$$p(E) = C \times e^{-E/a} \times \sinh(bE)^{1/2},$$

where a=0.965 MeV, b=2.29 MeV^{-1}.

Besides prompt particles from fission reactions, decay or delayed gammas from

fission products have some contribution to the energy depositions in reactor instruments. The prompt gammas can be accounted in the event of fission or neutron capture by nuclides but delayed gammas are not accounted by any nuclear processes in MCNP run. Thus to account the delayed gammas, additional photon transport calculation is performed by utilizing delayed gamma spectrum as source distribution. Table 2 shows the fission-products delayed gamma spectrum[7] with the total number of delayed gammas produced from one fission.

The total number of particles generated or incident upon MCNP problem geometry is necessary for the calculation of normalization factor or source. The reactor thermal output of 2815 MWth at normal full power operating condition is used for the calculation of total number of particles generated in the problem geometry.

MCNP utilizes a continuous form of ENDF/B cross-section library. In this calculation ENDF/B-VI cross sections are employed. Because the fuel and core internal temperatures are much higher than the library temperature (300 °K), the temperatures of each cell such as fuel pellet, cladding, core internals, etc. are input to consider the thermal motion of target nucleus. For incident neutron energies below about 4 eV, cross-section treatment for light water that takes into account the effects of chemical binding was employed by MCNP input option in the reactor coolant.

Sufficient number of particle histories of 1.2×10^7 was applied to MCNP runs to achieve good precision of the results, which gives the relative errors less than 0.002 on the overall heating rates results.

3. Results and Discussions

The heating rates of each component for CEA, ICI and NSA inside guide tube have been calculated by MCNP code. Table 3 shows heating rates of all component materials in two forms, one is per component volume and the other is per total volume of GT channel.

The heating rates have been compared with those from previous calculations as shown in Table 4. For ICI and NSA the heating rates have been obtained from System 80[3], while for CEA and PSCEA the heating rates have been obtained from YGN 3&4[5]. The comparisons of heating rates have been done per GT channel volume. The original data for System 80 have been provided as heating rates per volume of each component but unfortunately the volume data of each component are not available. Thus, the original data have been converted to heating rates per GT channel volume using material densities and KSNP mass data of each component

under the assumption that the masses of each component for System 80 are the same as those for KSNP.

The components of instruments for KSNP and System 80 are not exactly match to each other, so heating rates of similar component materials are coupled together for comparison, for example the heating rate of Inconel in ICI for System 80 represents that of Inconel and stainless steel.

As shown in Table 4, the rhodium heating rate for System 80 is very low compared to that for KSNP due to the fact that rhodium heating rate in ICI for System 80 had been derived as Inconel heating multiplied by density ratio of rhodium to Inconel[3]. But the quantity of rhodium in ICI is so small that the contribution of this difference is negligible.

Unlike the results of heating rates in ICI and NSA, the relative differences in total heating rates in CEA and PSCEA are somewhat larger. The previous methodology of CEA heating calculation was based on the heating factors classified by their origins of heating and the heating factors were multiplied by neutron absorption rate or average node power density around CEA. So the power condition of previous calculation is differ from that of MCNP calculation which employs fixed uniform source distribution. The maximum powers of 0.7879 and 1.1212 for rodded full strength CEA and PSCEA had been applied for YGN 3&4 CEA heating rate calculations.

As described in the previous calculation methodology, the CEA heating rate is directly affected by fuel pins surrounding each rodded waterhole. But in the MCNP calculation, there is no consideration for power depression of fuel pins around rodded waterhole. To include the effect of peripheral pin power, MCNP criticality calculations have been performed for various arrangements and insertions of CEAs to find peripheral pin powers similar to those used for YGN 3&4 CEA heating rates calculations as shown in Table 1. The arrangement with fully inserted CEAs has been determined as shown in Figure 3. Figure 4 shows the relative pin power densities surrounding four rodded GTs and one unrodded waterhole. The upper right and left CEAs have been chosen for the tallies of heating rates since the average powers of upper locations are closer to those for YGN 3&4.

The effective multiplication factor obtained from MCNP criticality calculation is slightly larger than 1.0, so the CEA heating rates should be scaled down to satisfy the calculated total fission energy released from the system is equal to a reference FA power of 15.904 MWth. The heating rates from delayed gammas have been derived by multiplying unrodded node-wise power to the delayed gamma heating rates from

fixed source MCNP calculation for consistency with YGN-3&4 calculations.

The results for CEA heating rate calculation are presented and compared with those for YGN 3&4 as shown in Table 5. As shown in the table, the relative differences for the CEA heating rates have been reduced by including peripheral pin powers to the MCNP calculation. But there are still noticeable differences in the CEA heating rates as compared to the results of other instruments. This is because that the power distribution simulated in this MCNP calculation is just an intra-assembly pin powers with relative box power density of 1.0. To get best-estimate results, relative box power densities for CEA and/or PSCEA insertion cases should be examined and included in the heating rates calculation.

The overall heating rates for the ICI and NSA are in good agreement with those of previous calculation. Although some components of the instruments have large relative differences in heating rates, they have negligible effect on the overall heating rates because of their small quantity.

The heating rates from MCNP calculation are based on the relative box power density of 1.0, so appropriate peaking factors or relative box power density should be included in the heating rates for the instruments when they are used for a specific reactor core.

REFERENCES

1. R. G. Shimko, “Heating Rates in Arkansas PLCEA Fingers, ” 6370-PHD-016, CE, Jan. 1976.
2. K. L. Hall, “Physics Data for CEA, ICI and Neutron Source Assembly Cooling Analyses for St. Lucie 2 Cycle 1, ” 13172-PHD-082, CE, Apr. 1982.
3. R. G. Shimko, “SYSTEM 80 ICI Heating Rates,” 3800-PHD-118, CE, Sep. 1979.
4. J. F. Briesmeister, “MCNP-A General Monte Carlo N-Particle Transport Code Version 4B, ”Los Alamos National Laboratory, LA-12625-M, Mar. 1997.
5. J. S. Song, “CEA Heating Rates for YGN-3/4 Initial Core Final Design, ” 10587-NE-048, KAERI, Rev.00, Dec. 1991.
6. “The Nuclear Design and Core Physics Characteristics of the Yonggwang Nuclear Power Plant Unit 5 Cycle 1, ” KNF-Y5ICD-01024, Rev.00, KNFC, Jul. 2001.
7. R. E. Maerker, “Gamma-Ray Characterization of the Two-year Irradiation Experiment Performed at the Poolside Facility, ” NUREG/CR-4039, ORNL, Jan. 1985.

Table 1 Node-wise Maximum Values for Powers and Fluxes

		Full Strength CEA	Part Strength CEA
Power	Unrodded	1.2099	1.2249
	Rodded	0.7879	1.1212
Rodded Flux	Fast	2.505×10^{14}	3.244×10^{14}
	Thermal	1.336×10^{13}	6.073×10^{13}

Table 2 Delayed Gamma Spectrum from U-235 Fission

Upper Energy [MeV]	Delayed Gamma Spectrum	Source Probability
14.00	0.00E+00	0.000E+00
10.00	0.00E+00	0.000E+00
8.00	2.50E-04	3.570E-05
7.00	5.00E-04	7.140E-05
6.00	6.90E-03	9.853E-04
5.00	3.89E-02	5.555E-03
4.00	4.17E-02	5.955E-03
3.00	3.41E-01	4.869E-02
2.00	3.36E-01	4.798E-02
1.50	1.10E+00	1.571E-01
1.00	7.88E-01	1.125E-01
0.80	4.75E-01	6.783E-02
0.70	6.47E-01	9.239E-02
0.60	1.14E+00	1.628E-01
0.40	1.14E+00	1.628E-01
0.20	7.05E-01	1.007E-01
0.10	1.08E-01	1.542E-02
0.06	8.08E-02	1.154E-02
0.03	2.69E-02	3.841E-03
0.02	2.69E-02	3.841E-03
Sum	7.0	1.0

Table 3 Heating Rates for CEA, ICI and NSA

CEA Component	Heating Rate [W/cc]			
	per component			per GT channel
	Prompt	Delayed	prompt+delayed	
B_4C	26.28	0.53	26.81	14.58
Inconel-625	8.81	2.66	11.47	1.32
SS 347	7.72	2.32	10.05	0.09
H_2O	3.67	0.24	3.91	0.63
Zircaloy-4	8.38	2.29	10.67	1.67
Channel Average	17.28	1.01	18.29	18.29

PSCEA Component	Heating Rate [W/cc]			
	per component			per GT channel
	Prompt	Delayed	prompt+delayed	
Inconel-625	10.67	2.29	12.96	8.83
H_2O	3.84	0.22	4.06	0.66
Zircaloy-4	9.64	2.14	11.78	1.84
Channel Average	9.40	1.93	11.33	11.33

ICI Component	Heating Rate [W/cc]			
	per component			per GT channel
	prompt	delayed	prompt+delayed	
^{103}Rh	727.08	4.78	731.86	0.13
Inconel-600	10.18	2.63	12.82	1.48
Al_2O_3	4.65	1.11	5.76	0.08
H_2O	3.82	0.24	4.07	2.57
Zircaloy-4	9.20	2.29	11.49	1.80
Channel Average	5.23	0.83	6.06	6.06

NSA Component	Heating Rate [W/cc]			
	per component			per GT channel
	prompt	delayed	prompt+delayed	
Pd-Cf_2O_3	49.49	4.32	53.81	9.5E-04
Sb-Be	15.43	1.28	16.71	0.78
SS	8.83	2.32	11.15	1.99
Inconel X-750	10.45	2.57	13.02	0.04
H_2O	3.85	0.25	4.09	1.66
Zircaloy-4	9.32	2.28	11.60	1.82
Channel Average	5.35	0.94	6.29	6.29

Note : Radial and axial peaking factors of 1.0 were used and no uncertainties were included on the results.

Table 4 Comparisons of Heating Rates

CEA Component	Heating Rate [W/cc]		Relative Difference [%]
	MCNP[(a)]	YGN 3&4	
B_4C	14.58	13.10	10.2
Inconel	1.41[(b)]	1.42	-1.1
H_2O	0.63	0.49	21.9
Zircaloy-4	1.67	1.69	-0.9
Total	18.29	16.70	8.7

PSCEA Component	Heating Rate [W/cc]		Relative Difference [%]
	MCNP	YGN 3&4	
Inconel	8.83	10.70	-21.2
H_2O	0.66	0.76	-16.0
Zircaloy-4	1.84	2.45	-32.8
Total	11.33	13.91	-22.8

ICI Component	Heating Rate [W/cc]		Relative Difference [%]
	MCNP	System 80	
^{103}Rh	0.13	3.8E-03	97.1
Inconel	1.48	1.52[(b)]	-3.2
Al_2O_3	0.08	0.09	-8.3
H_2O	2.57	3.03	-17.9
Zircaloy-4	1.80	1.75	2.7
Total	6.06	6.40	-5.6

NSA Component	Heating Rate [W/cc]		Relative Difference [%]
	MCNP	System 80	
Pd-Cf_2O_3 or Pu-Be	9.5E-04	8.6E-04	9.9
Sb-Be	0.78	0.28	64.1
SS	1.99	2.23[(c)]	-12.1
Inconel	0.04	0.04	3.6
H_2O	1.66	2.34	-40.9
Zircaloy-4	1.82	1.68	7.4
Total	6.29	6.57	-4.5

Note : Radial and axial peaking factors of 1.0 were used on the calculations except for YGN 3&4 CEA and PSCEA heating rates calculations, and no uncertainties were included on the results.

(a) Results for KSNP from MCNP calculations

(b) Inconel + Stainless Steel (c) Stainless Steel + Aluminum

Table 5 Comparisons of CEA Heating Rates with Modified MCNP Results

CEA	Heating Rate [W/cc]		Relative Difference [%]
	MCNP[(a)]	YGN 3&4	
Full Strength	17.63	16.70	5.3
Part Strength	12.02	13.91	-15.7

Note : No uncertainties were included on the results.

(a) Heating = (scale factor)×(prompt heating)+(unrodded power)×(delayed γ heating)

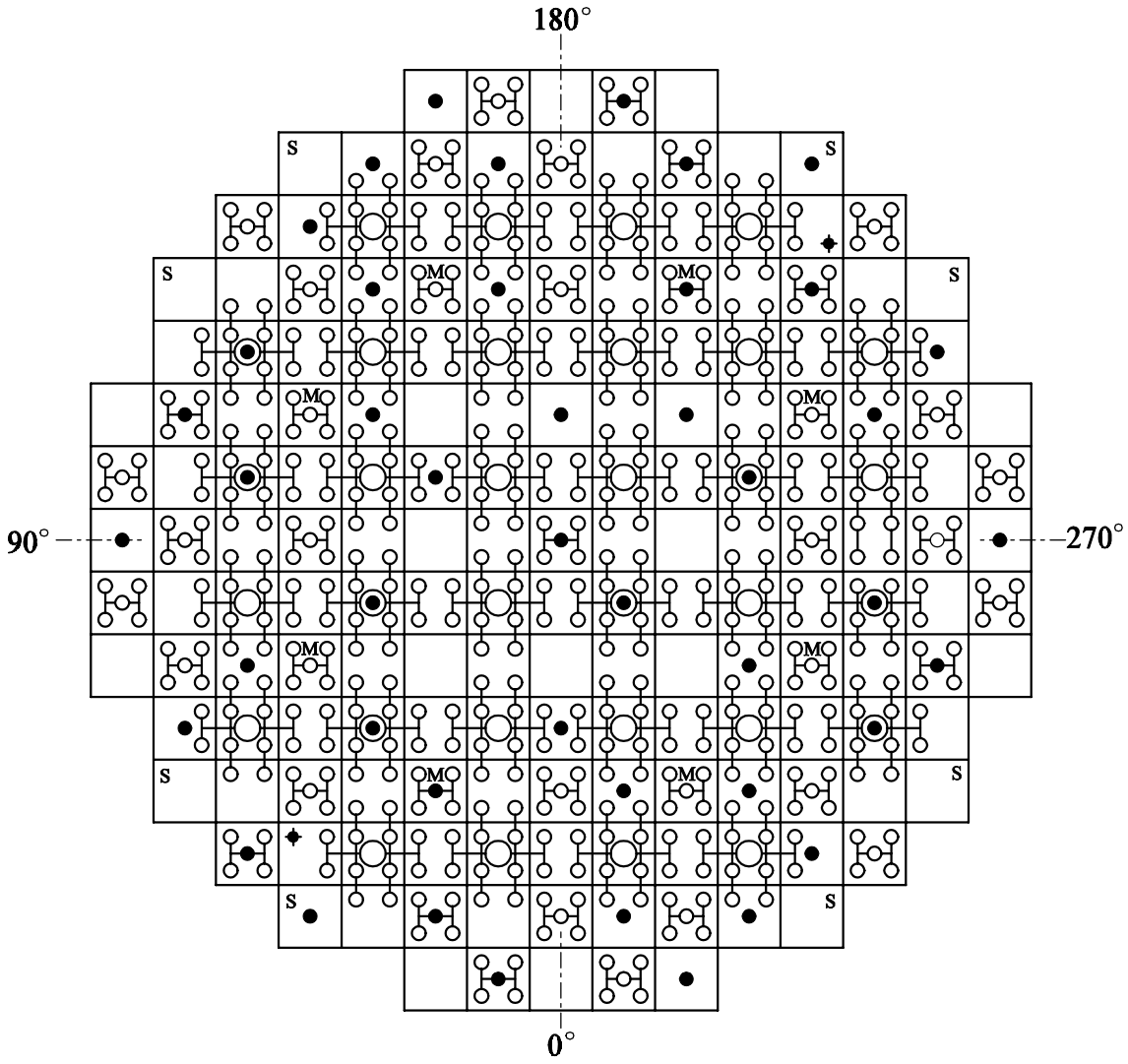

Figure 1 Control Element Assembly and In-Core Instument Locations

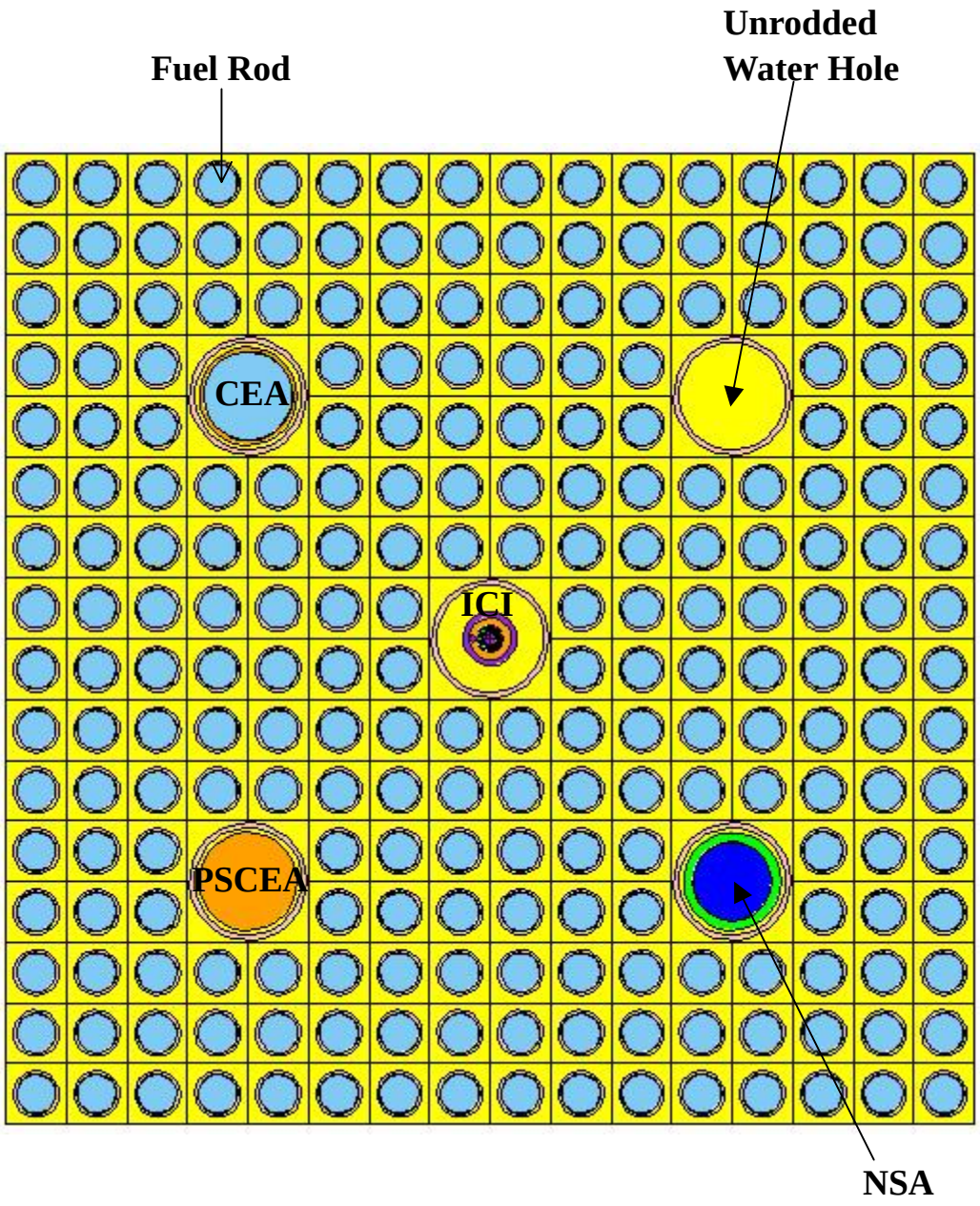

Figure 2 Cross Sectional View of MCNP Model at Core Mid-Plane

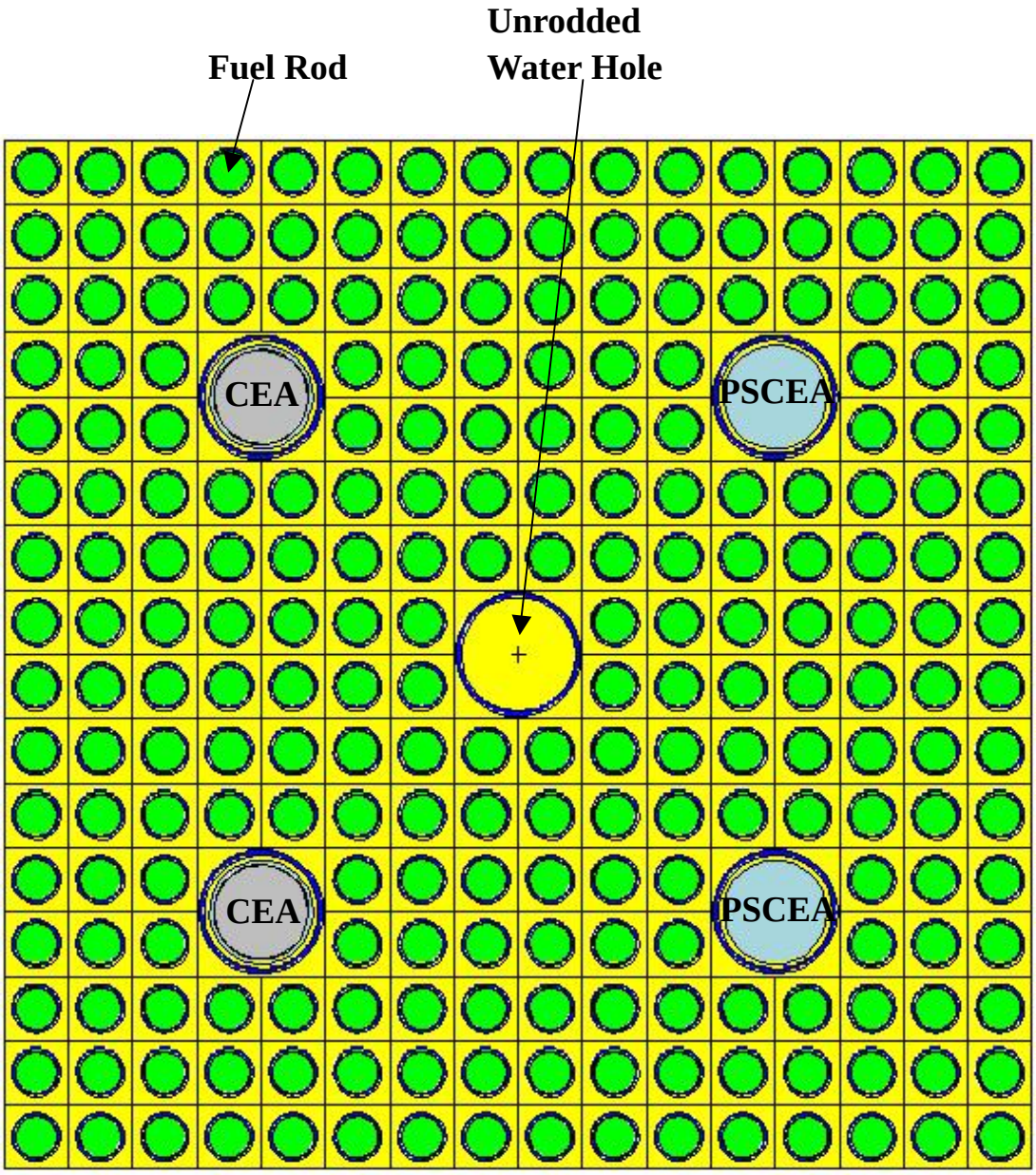

Figure 3 Cross Sectional View of MCNP Model for Criticality Calculation at Core Mid-Plane

a. Relative Pin Power Distribution

0.880	0.884	0.887	0.863	0.871	0.933	0.965	0.975	1.061	1.063	1.100	1.111	1.128	1.137	1.114	1.162
0.900	0.856	0.852	0.842	0.827	0.898	0.943	1.007	1.043	1.076	1.061	1.093	1.101	1.133	1.159	1.186
0.867	0.846	0.786	0.743	0.755	0.839	0.940	0.998	1.039	1.102	1.061	1.063	1.095	1.123	1.157	1.157
0.861	0.847	0.755			0.770	0.899	0.972	1.055	1.076	1.056			1.117	1.143	1.153
0.856	0.794	0.745			0.807	0.945	1.014	1.067	1.072	1.071			1.110	1.110	1.160
0.875	0.858	0.810	0.762	0.770	0.876	1.002	1.068	1.097	1.089	1.122	1.118	1.112	1.124	1.139	1.104
0.908	0.881	0.865	0.833	0.877	0.981	1.042	1.190	1.219	1.166	1.137	1.126	1.115	1.116	1.124	1.131
0.881	0.877	0.847	0.907	0.950	1.028	1.166			1.262	1.149	1.136	1.114	1.124	1.113	1.117
0.916	0.919	0.865	0.901	0.948	1.008	1.173			1.292	1.139	1.127	1.138	1.129	1.128	1.134
0.871	0.863	0.870	0.843	0.900	0.942	1.054	1.153	1.228	1.180	1.131	1.122	1.106	1.120	1.097	1.166
0.865	0.849	0.800	0.740	0.791	0.875	0.984	1.043	1.096	1.139	1.111	1.084	1.097	1.092	1.113	1.147
0.882	0.816	0.732			0.785	0.919	0.983	1.046	1.058	1.045			1.095	1.118	1.157
0.843	0.815	0.712			0.782	0.910	0.976	1.009	1.058	1.057			1.075	1.115	1.154
0.865	0.857	0.796	0.694	0.740	0.831	0.936	0.969	1.018	1.046	1.045	1.055	1.058	1.107	1.103	1.124
0.883	0.871	0.849	0.790	0.859	0.902	0.947	1.026	1.019	1.037	1.094	1.095	1.071	1.108	1.110	1.135
0.898	0.862	0.869	0.869	0.878	0.943	0.979	1.038	1.043	1.040	1.088	1.072	1.102	1.128	1.132	1.144

b. Average Power Density of the 12 Fuel Pins Surrounding each Waterhole

0.785		1.098
	1.177	
0.773		1.077

Figure 4 Relative Pin Power Distribution from MCNP Criticality Calculation